Demonstration of HOT photoresponse of MWIR T2SLs InAs/InAsSb photoresistors

K. MICHALCZEWSKI[1]*, T. Y. TSAI[2], P. MARTYNIUK[1], and C.H. WU[2]

[1] Institute of Applied Physics, Military University of Technology, 2 Urbanowicza Str., 00-908 Warsaw, Poland
[2] Graduate Institute of Photonics and Optoeletronics, National Taiwan University, Roosevelt Str., 10617 Taipei, Taiwan

Abstract. We report on the photoresponse of mid-wavelength infrared radiation (MWIR) type-II superlattices (T2SLs) InAs/InAsSb high operating temperature (HOT) photoresistor grown on GaAs substrate. The device consists of a 200 periods of active layer grown on GaSb buffer layer. The photoresistor reached a 50% cut-off wavelength of 5 μm and 6 μm at 200 K and 300 K respectively. The time constant of 30 ns is observed at 200 K under 1 V bias. This is the first observation of the photoresponse in MWIR T2SLs InAs/InAsSb above 200 K..

Key words: HOT, MWIR T2SLs InAs/InAsSb, photoresistor.

1. Introduction

From the physics point of view type-II superlattices (T2SLs) are interesting material. The fundamental lower Auger recombination [1], stronger bonds and structural stability [2], lower band-to-band tunnelling due to larger electron effective mass [3], as well as growth and *processing* technology [4] make T2SLs a potential candidate to replace expensive HgCdTe and to operate at higher temperatures. T2SLs InAs/InAs$_{1-x}$Sb$_x$ and InAs/GaSb concept have been widely studied over last 2 decades. Due to the fact that minority carrier lifetime in InAs/GaSb T2SLs is limited by Shockley-Read-Hall (SRH) mechanism, the InAs/InAs$_{1-x}$Sb$_x$ T2SLs material is considered as alternative for infrared laser and detector application. The absence of Gallium (Ga) being responsible for above mentioned recombination centers allows T2SLs InAs/InAsSb to have much longer lifetimes, up to 10 μs for undoped material in mid-wavelength infrared radiation (MWIR) region [5].

GaSb substrate is the best choice to grow T2SLs on due to its lattice constant being between InAs and InAsSb [6]. From the other point of view in order to produce cheap infrared focal plane arrays (IR FPAs) it is recommended to utilize GaAs substrate. GaAs has better structural, optical and thermal properties than GaSb. In addition, these substrates are more affordable and available as large size "epi-ready" wafers up to 6 inch in diameter. Transparent GaAs substrate allows for the backsided device illumination and fabrication of monolithic optical immersion [7].

The interfacial misfit array (IMF) is the best technique which allows to reach a high quality GaSb buffer layer on GaAs substrate. In IMF the mismatch between GaSb and GaAs is accommodated at the interface by formed a 2D periodic array of 90° dislocation (Lomer dislocation) along both [110] and [1–10] direction [8]. In this paper, InAs/InAsSb T2SLs grown by molecular beam epitaxy (MBE) is studied. High-resolution X-ray diffraction (HRXRD), optical characterizations made of photoluminescence (PL), spectral response and response time measurements performed on InAs/InAsSb T2SLs are reported and analyzed.

2. Growth description

The T2SLs InAs/InAsSb layers were grown by a RIBER Compact 21-DZ solid source MBE system, on GaAs (001) substrates. The system is equipped with double filament effusion cells for Ga and In, and with valved cracker cells for As and Sb. As$_2$ and Sb have been used. The manipulator thermocouple was used to monitor the substrate temperature. Growth temperature was calibrated from the GaAs substrate deoxidization temperature. After the deoxidation of the GaAs substrate at 675°C under As$_2$ overpressure, a 250 nm-thick GaAs layer was first deposited at 655°C to smooth the substrate surface. The reflection high-energy electron diffraction (RHEED) surface reconstruction showed a 2×4 pattern characteristic for a As-rich surface. Afterwards in order to reach Ga rich surface the Ga shutter was closed to let the As adatoms desorb. When the 4×2 GaAs surface reconstruction was generated the substrate temperature was reduced to 505°C under Sb overpressure. The reconstruction of the surface transformed to a 2×8 revealing that the Sb adatoms have combined with Ga rich surface. After stabilization of the temperature at 505°C the Ga shutter was opened and the GaSb layer growth started. Instantaneously the spotty RHEED pattern appeared at the growth of the first few monolayers indicating a 3D growth mode. Subsequently after next few monolayers the 1×3 surface reconstruction was generated indicating a 2D growth mode. The thickness of GaSb buffer layer was set to be ∼ 1.0 μm. The growth rate for the GaSb layer was 0.76 μm/h while the BEP (beam equivalent pressure) group V/III flux ratio (Sb/Ga) was set to be 5. Then the substrate was cooled down

to 425°C under Sb overpressure. When the temperature was stabilized the T2SLs growth started. During the growth short soaking of As and As + Sb time was used to minimize surface composition changing at the interfaces. The growth rate of InAs layer was set to 0.5 ML/s and InAsSb ~ 0.53 ML/s. Prior to the growth the calibration processes were performed to reach required composition of InAsSb layer. Strain calculation was evaluated by equation from work by Polly *et al.* [9].

3. High-resolution X-ray diffraction (HRXRD)

X-ray diffractometer of PANalytical X'Pert was utilized to assess the structural properties of the InAs/InAsSb T2SLs. The Cu Kα_1 radiation ($\lambda = 1.5406$ Å) originating from a line focus was used. The X-ray beam was monochromatized by four bounce, Ge (004) hybrid monochromator. The measurements were performed in 2Θ-ω direction. Figure 1a represents the high-resolution X-ray diffraction pattern around the symmetric 004 reflection of 200 periods with simulation made by PAN-

alytical software. The full-width at half-maximum (FWHM) of the zeroth-order peak (2Θ-ω) is equal to 147 arcsec. In Fig. 1a, the 2Θ-ω scan shows two diffraction peaks, at the position 2Θ = 66.07° and 2Θ = 60.73°, corresponding to GaAs substrate and GaSb buffer layer, respectively. The strain balance has not been reached for that sample. The sample is in tensile mismatch in the growth direction. Figure 1b presents the architecture of T2SLs InAs/InAsSb.

4. Photoluminescence (PL) measurements

The PL emission was analyzed using a Bruker Vertex v70 Fourier transform infrared (FTIR) spectrometer. The sample was placed in a closed cryostat, that allows a precise control of the temperature from 40 K to 300 K. 630 nm diode with mechanical chopper was used to the sample excitation the sample through a CaF$_2$ window. The whole optical path was under vacuum conditions. The PL spectra measurements from 80 K to 300 K are presented in Fig. 2a. For each temperature, the PL energy peak
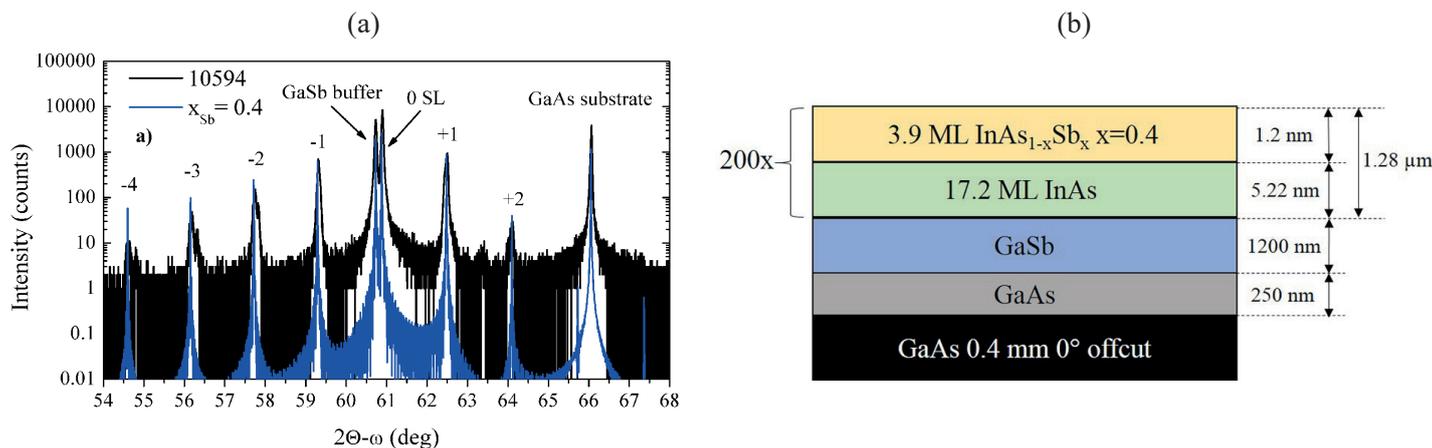
(a) (b)

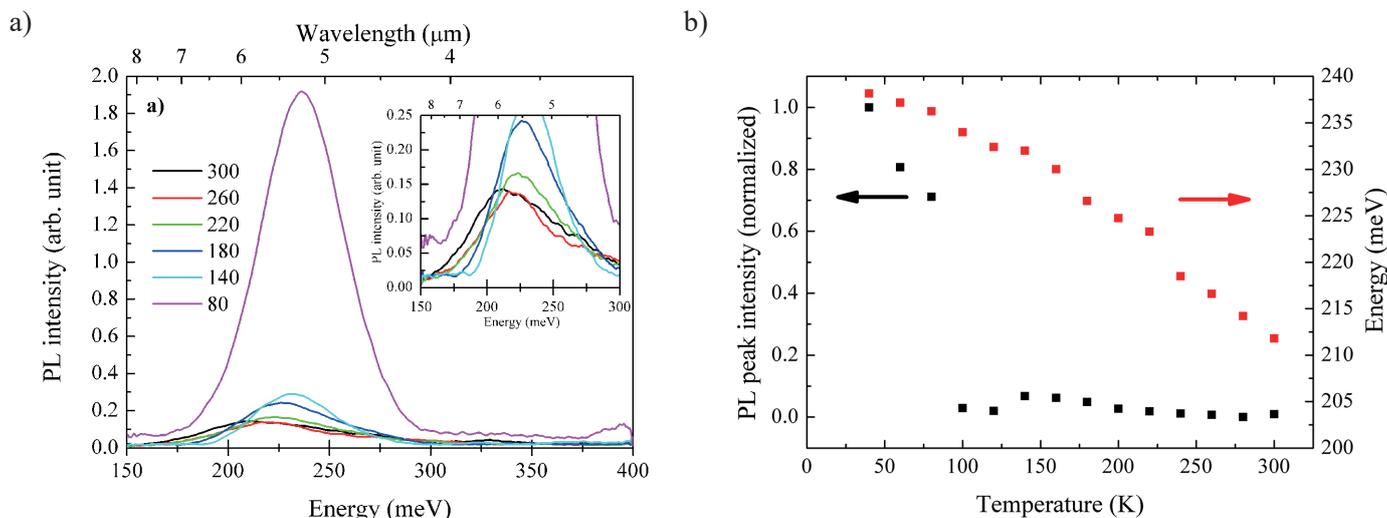Fig. 1. HRXRD spectrum with simulation of T2SLs (a), T2SLs InAs/InAsSb sample schematic cross section (b)

Fig. 2. PL spectra intensity for selected temperatures: 80–300 K (a), energy peak value and normalized intensity (b) for analyzed T2SLs InAs/InAsSb
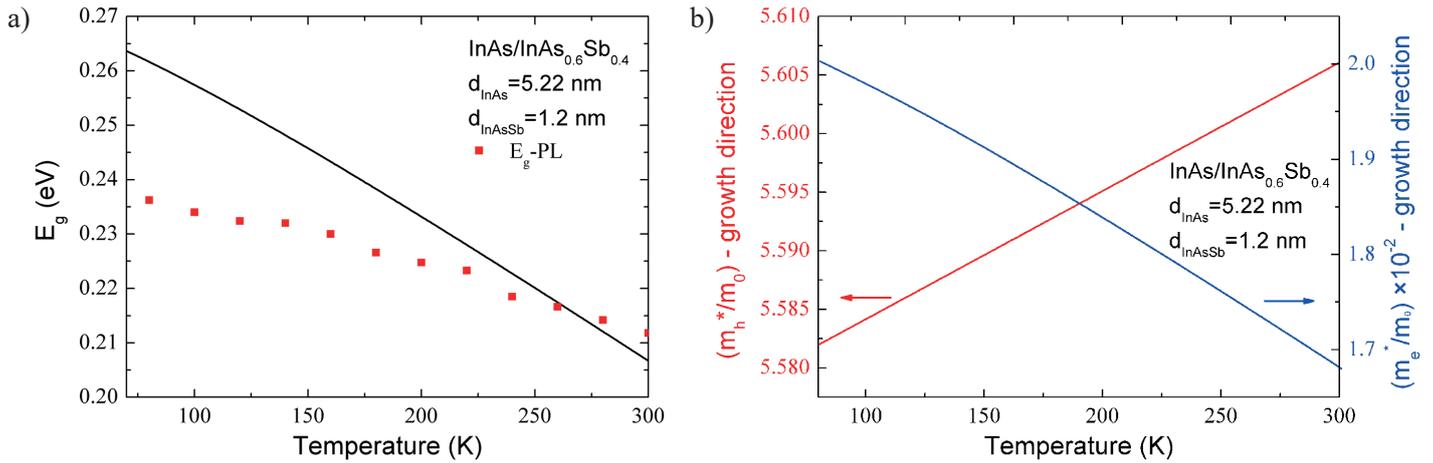
a)

b)

Fig. 3. kp calculated, PL measured bandgap versus temperature (a), growth direction electron and hole effective mass for T2SLs InAs (5.22 nm)/ InAs$_{0.6}$Sb$_{0.4}$(1.2 nm) (b).
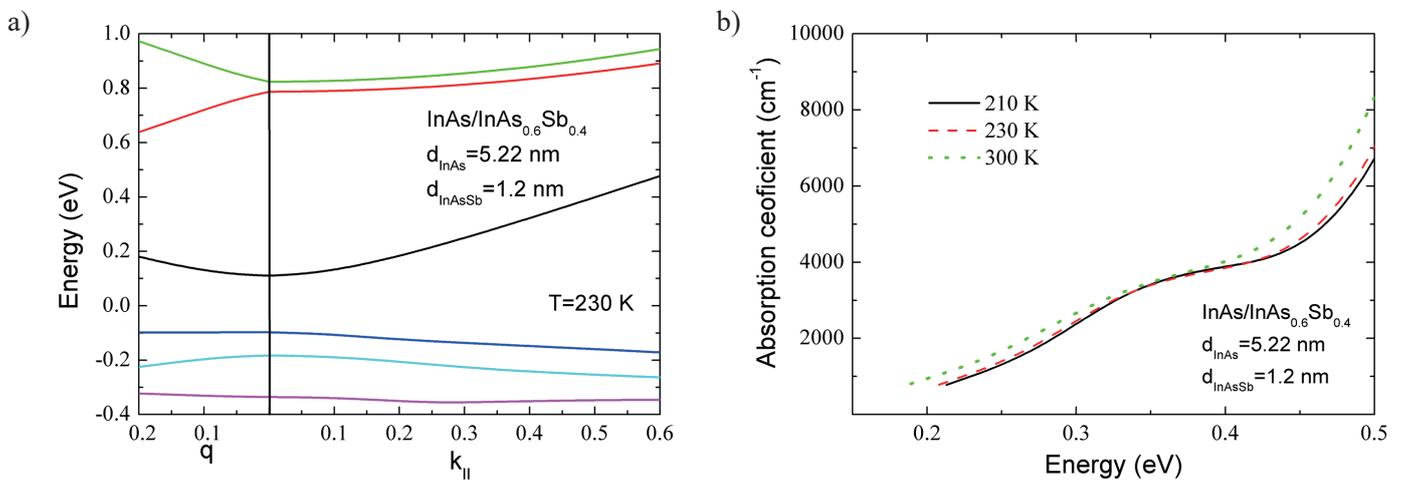
a)

b)

Fig. 4. Dispersion curves in plane and growth direction (a), calculated absorption coefficient for selected temperatures: $T = 210$; 230 and 300 K (b) for InAs (5.22 nm)/InAs$_{0.6}$Sb$_{0.4}$(1.2 nm)

value and intensity was extracted and plotted in Fig. 2b. The FWHM of the peak at 80 K is equal to 49 meV. From the shape of the normalized intensity relation (Fig. 2b) we can conclude that at range of temperature from 100 K to 300 K the performance of the photoconductor is limited.

Referring to Olson *et al*. work the dominant recombination mechanism in undoped T2SLs for temperatures higher than 200 K is Auger recombination [10]. Durlin *et al*. showed that in MWIR T2SLs InAs/InAsSb below 200 K the dominant recombination mechanism is SRH [11].

5. Analysis of the T2SLs InAs/InAsSb band structure

The kp method was used to calculate band structure, absorption coefficient and band gap. The E-k relation of InAs (5.22 nm)/ InAs$_{0.6}$Sb$_{0.4}$ (1.2 nm) is presented in Fig. 4a. Figure 3 represent the calculated band gap in comparison with photolumi-

nescence measurement. The results were in proper agreement with simulation. The best fitting was reached at higher operating temperature (HOT) range $T > 225$ K. The higher absorption coefficient at 300 K can be explained by the allowed higher subband transitions at this temperature.

Table 1a
Fractional band offsets for T2SLs InAs/InAsSb.

Fractional conduction band offset	Q_c	2.3
Fractional valence band offset	Q_c	−1.3

Table 1b
Bowing parameters InAsSb

	E_g^Γ(eV)	0.67
Bowing parameters	Δ_0(eV)	1.2
	$m_e^*(\Gamma)$	0.035

K. Michalczewski, T.Y. Tsai, P. Martyniuk, and C.H. Wu

Table 1c
Material parameters taken in modeling of T2SLs InAs/InAsSb

Parameters	Symbols	GaAs	InAs	InSb	GaSb
Lattice constant $a(T) = a(T = 300\,K) + \alpha_T \times (T\text{-}300)$	$a_T(\text{Å}/K)$	3.88×10^{-5}	2.74×10^{-5}	3.48×10^{-5}	4.72×10^{-5}
	$a(T = 300\,K)(\text{Å})$	5.65325	6.0583	6.4794	6.0959
Band Gap $E_g^\Gamma(T) = E_g^\Gamma(T = 0\,K) - \dfrac{\alpha T^2}{T+\beta}$	$\alpha(\text{meV}/K)$	0.5405	0.276	0.32	0.417
	$\beta(K)$	204	93	170	140
	$E_g^\Gamma(T = 0\,K)(\text{eV})$	1.519	0.417	0.25	0.812
Luttinger parameters	γ_1	7.05	20.0	34.8	13.4
	γ_2	2.35	8.5	15.5	4.7
	γ_3	3	9.2	16.5	6
Deformation potentials	$a_c(\text{eV})$	-7.17	-5.08	-6.94	-7.5
	$a_v(\text{eV})$	-1.16	-1	-0.36	-0.8
	$b(\text{eV})$	-2	-1.8	-2	-2
	$d(\text{eV})$	-4.8	-3.6	-4.7	-4.7
Elastic constant	$C_{11}(\text{GPa})$	1221	832.9	684.7	884.2
	$C_{12}(\text{GPa})$	566	452.6	373.5	402.6
	$C_{44}(\text{GPa})$	600	395.9	311.1	432.2
Spin-orbit energy	$\Delta_0(\text{eV})$	0.341	0.39	0.82	0.76
Kane potential	$E_p(\text{eV})$	23.81	21.5	24.08	24.76
Electron affinity	(eV)	4.07	4.9	4.59	4.06
Valence band offset	VBO(eV)	-0.8	-0.59	0	-0.03
Effective mass (0 K)	$\dfrac{m_e^*}{m_0}$	0.064	0.023	0.0138	0.038

6. Spectral and time constant measurements

The front side illuminated SL photoconductor was utilized with 100×90 µm active region placed on 3-stage thermoelectric cooler. Figure. 5 shows the measured spectral responsivity of 200 periods InAs/InAsSb photoconductor at HOT conditions. The device has 50% cut-off at 5.7 µm, 5.4 µm, 5.0 µm at 300 K, 230 K, 200 K respectively. The current responsivity R_i (3 µm) is equal to 0.2 A/W under 1 V bias. Detector resistance is 55 Ω at 200 K, therefore the applied bias voltage correspond to current power supply of 18 mA. The differences with PL measurement occur due to the thin active region of photoconductor. The highest responsivity was at 200 K which is in agreement with earlier PL measurements where the PL signal intensity was increasing from 300 K to 80 K. Heretofore minimal reports of spectral response have been published for T2SLs InAs/InAsSb and none were found for HOT conditions. The normalized spectral responsivity under 1 V bias compared to commercially available HgCdTe photoresistor is ~ 30 times lower at 200 K. It worth to noticing that the absorber thickness and doping has not been optimized yet.
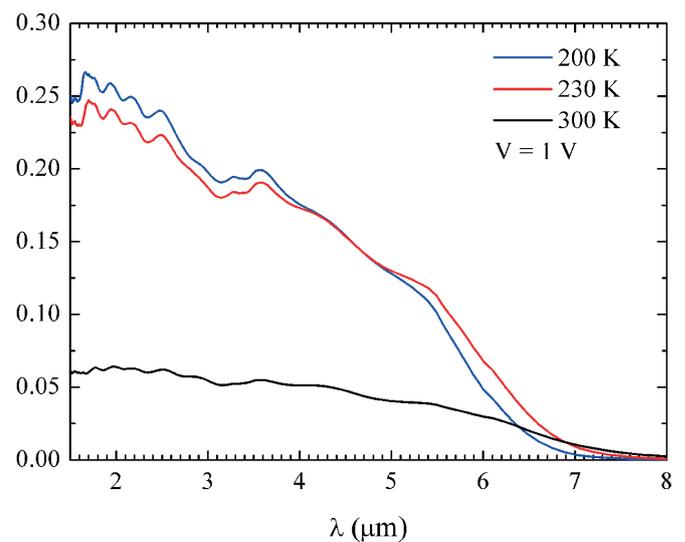

Fig. 5. Spectral responsivity of T2SLs InAs (5.22 nm)/InAs$_{0.6}$Sb$_{0.4}$ (1.2 nm) photodetector for selected temperatures $T = 200$; 230 and 300 K and $V = 1$ V.

The time constant was measured with an Optical Parametric Oscillator (OPO) as the source of ~25 ps pulses of infrared radiation, tunable in a 1.55–16 µm spectral range. In Table 2 the results are summarized. The time constant has reached maximum in 200 K and it is constant to 230 K. The same trend has been observed in Durlin *et al*. work [11]. In their work the longest carrier lifetimes was observed at range of temperature from 190 K to 230 K.

Table 2
Time constant results for voltage $V = 1$ V.

Temperature (K)	Time constant (ns)
300	11
230	30
200	30

7. Conclusion

In conclusion, a 200 periods T2SLs InAs/InAsSb photoconductor has been grown for MWIR detection and HOT condition. The first report of spectral response above 200 K was shown indicating potential of the T2SLs InAs/InAsSb material for HOT detectors. The structure exhibits 50% cut-off equal to 5 µm at 200 K. The PL measurements analysis revealed that the performance of the detector is limited up to 200 K mainly by Auger recombination. It should be noted that T2SLs InAs/InAsSb growth and material properties have not been optimized yet.

REFERENCES

[1] M.A. Kinch, Fundamentals of infrared detector materials, SPIE Press 2007.

[2] G. Osbourn, L. Dawson, R. Biefeld, T. Zipperian, I. Fritz, and B. Doyle, "III–V strained layer supperlattices for long-wavelength detector applications: Recent progress", *Journal of Vacuum Science & Technology A: Vacuum, Surfaces, and Films* 5, 3150–3152 (1987).

[3] J. Schulman and T. McGill, "The CdTe/HgTe superlattice: Proposal for a new infrared material", *Appl. Phys.Lett.* 34, 663–665 (1979).

[4] Y. Huang, J. Ryou, R. Dupuis, V. D'costa, E. Steenbergen, and J. Fan, et al. "Epitaxial growth and characterization of InAs/GaSb and InAs/InAsSb type-II superlattices on GaSb substrates by metalorganic chemical vapor deposition for long wavelength infrared photodetectors", *J. Cryst. Growth.* 314, 92–96 (2011).

[5] A. Rogalski, M. Kopytko, and P. Martyniuk, "InAs/GaSb type-II superlattice infrared detectors: future prospect", *App. Phys. Rev.* 4.3, 031304 (2017).

[6] J. Bajaj, G. Sullivan, D. Lee, E. Aifer, and M. Razeghi, "Comparison of type-II superlattice and HgCdTe infrared detector technologies", *Proc. SPIE* 65420, 65420B (2007).

[7] K. Michalczewski, F. Ivaldi, Ł. Kubiszyn, D. Benyahia, J. Boguski, and A. Kębłowski, et al. "Studies of dark current reduction in InAsSb mid-wave infrared HOT detectors through Two step passivation technique", *Acta Physica Polonica A.* 132, 325–328 (2017).

[8] D. Benyahia, K. Michalczewski, A. Kębłowski, P. Martyniuk, J. Piotrowski, and A. Rogalski, „Interfacial misfit array technique for GaSb growth on GaAs (001) substrate by molecular beam epitaxy", *J Electron Mater.* 47, 299–304 (2017).

[9] S.J. Polly, C.G. Bailey, A.J. Grede, D.V. Forbes, and S.M. Hubbard, "Calculation of strain compensation thickness for III–V semiconductor quantum dot superlattices", *J.Cryst.Growth.* 454, 64–70 (2017).

[10] B. Olson, E.A. Shaner, J.K. Kim, J.F. Klem, S.D. Hawkins, and M. Flatté, et al. "Identification of dominant recombination mechanisms in narrow-bandgap InAs/InAsSb type-II superlattices and InAsSb alloys", *Appl. Phys. Lett.* 103, 052106 (2013).

[11] Q. Durlin, J. Perez, R. Rossignol, J. Rodriguez, L. Cerutti, and B. Delacourt, et al., "InAs/InAsSb superlattice structure tailored for detection of the full midwave infrared spectral domain", *Quantum sensing and nano electronics and photonics XIV, International Society for Optics and Photonics*, 10111, 1011112 (2017).